Supporting Information

Nanoporous Zn^{II}/Tb^{III}-Organic Frameworks for CO_2 Conversion

*Hongtai Chen, Liming Fan, Xiutang Zhang**

Department of Chemistry, College of Science, North University of China, Taiyuan 030051, People's Republic of China. E-mail: xiutangzhang@163.com.

Table S1. Crystallographic data and refinement parameters of NUC-7.

Complex	**NUC-7**
Formula	$C_{40}H_{44}ZnN_5O_{19}Tb$
Mr	1123.11
Crystal system	trigonal
Space group	R-3m
a (Å)	47.9295(17)
b (Å)	47.9295(17)
c (Å)	13.1746(4)
α (°)	90
β (°)	90
γ (°)	120
V(Å^3)	26210(2)
Z	18
Dcalcd(g·cm^{-3})	0.921
μ(mm^{-1})	1.651
GOF	1.002
R_1 [I＞2σ(I)]a	0.0711
wR_2 [I＞2σ(I)]b	0.2165
R_1[a](all data)	0.0948
wR_2[b] (all data)	0.2441
R_{int}	0.1562

[a] $R_1 = \sum| |F_o|-|F_c| | / \sum|F_o|$. [b] $wR_2 = [\sum w(|F_o^2|-|F_c^2|)/\sum|w(F_o^2)^2|]^{1/2}$

Table S2. Selected bond lengths and angles.

NUC-7					
Zn1-O3	1.9051(69)	Zn1-O8#2	1.9586(81)	Zn1-O8#3	1.9596(53)
Zn1-O1#1	1.9331(66)				
Tb1-O4#5	2.3241(79)	Tb1-O1W	2.3724(70)	Tb1-O5#8	2.4996(68)
Tb1-O7#4	2.2720(52)	Tb1-O6#6	2.4076(63)	Tb1-O6#7	2.4080(58)
Tb1-O7	2.2725(53)				
#1 4/3-x, 2/3-x+y, 5/3-z; #2 2/3-x+y, 4/3-x, 1/3+z; #3 2/3-x+y, 1/3+y, 1/3+z; #4 1-y, 1-x, z; #5 4/3-y, 2/3+x-y, -1/3+z; #6-1/3+y, 1/3-x+y, 1/3-z; #7 2/3+x-y, 4/3-y, 1/3-z; #8 -1/3+y, 1/3-x+y, 1/3-z;					
O1#3-Zn1-O8#6	103.01(18)	O1#3-Zn1-O8#6	103.01(18)	O3-Zn1-O1#3	99.0(3)
O3-Zn1-O8#4	116.65(17)	O3-Zn1-O8#6	116.65(17)	O8#4-Zn1-O8#6	114.8(3)
O4#5-Tb1-O5#8	124.92(18)	O4#5-Tb1-O5#7	124.92(18)	O4#5-Tb1-O6#7	74.18(19)
O4#5-Tb1-O6#8	74.18(19)	O4#5-Tb1-O1W	152.0(3)	O5#7-Tb1-O5#8	81.6(4)
O6#8-Tb1-O5#8	51.7(2)	O6#7-Tb1-O5#7	51.7(2)	O6#8-Tb1-O5#7	102.9(2)
O6#7-Tb1-O5#8	102.9(2)	O6#7-Tb1-O6#8	80.3(3)	O7-Tb1-O4#5	79.9(2)
O7#9-Tb1-O4#5	79.9(2)	O7#9-Tb1-O5#8	154.0(2)	O7-Tb1-O5#8	90.0(2)
O7#9-Tb1-O5#7	90.0(2)	O7-Tb1-O5#7	154.0(2)	O7#9-Tb1-O6#8	154.0(2)
O7-Tb1-O6#7	154.0(2)	O7#9-Tb1-O6#7	90.6(2)	O7-Tb1-O6#8	90.6(2)
O7-Tb1-O7#9	87.0(3)	O7-Tb1-O1W	79.9(2)	O7#9-Tb1-O1W	79.8(2)
O1W-Tb1-O5#7	74.2(2)	O1W-Tb1-O5#8	74.2(2)	O1W-Tb1-O6#8	125.1(2)
O1W-Tb1-O6#7	125.1(2)				
#1 2/3-Y+X,1/3+X,1/3-Z; #2 +X,1+X-Y,+Z; #3 4/3-X,5/3-Y,5/3-Z; #4 2/3+Y-X,4/3-X,1/3+Z; #5 4/3-Y,2/3+X-Y,-1/3+Z; #6 2/3+Y-X,1/3+Y,1/3+Z; #7 -1/3+Y,1/3-X+Y,1/3-Z; #8 2/3-Y+X,4/3-Y,1/3-Z; #9 1-Y,1-X,+Z.					

Table S3. Comparison of Cycloaddition of CO_2 with styrene oxide.[a]

Entry	Catalyst	Yield %	Ref.
1	Zn-NTTA	64.1	S1
2	$\{[Zn_2(3\text{-tpom})(L)_2]\cdot 2H_2O\}n$	78	S2
3	$\{[PMo_8{}^{V}Mo_4{}^{VI}O_{37}(OH)_3Zn_4][BPE]_2\}\cdot[BPE]$	96	S3
4	$[Zn(L2)(x)_{0.5}]\cdot 0.5H_2O$	80	S4
5	$[Zn_4O(2,6\text{-NDC})(BTB)_{4/3}]$	58	S5
6	$[Zn_2(TCA)(BIB)_{2.5}]\cdot(NO_3)$	51.3	S6
7	Zn(Bmic)(AT)	98	S7

[a]Reaction condition: in a typical reaction, styrene oxide (20 mmol), MOF/catalyst (1 mol%), 1 atm CO_2, TBAB (5 mol%), 80 ^{o}C

Table S4. The K_{sv}values of selected luminescent Ln-MOFs materials for detection of Fe^{3+}.

Ln-MOF	**substrates**	K_{sv}	**Ref.**
Eu−HODA	Fe^{3+}	2.09×10^4 M^{-1}	S8
Complex **2**	Fe^{3+}	4.30×10^4 M^{-1}	S9
Complex **1**	Fe^{3+}	1.66×10^4 M^{-1}	S10
Complex **2a**	Fe^{3+}	3.10×10^4 M^{-1}	S11
Eu-3	Fe^{3+}	4.30×10^4 M^{-1}	S12
NUC-7	Fe^{3+}	4.77×10^4 M^{-1}	This work

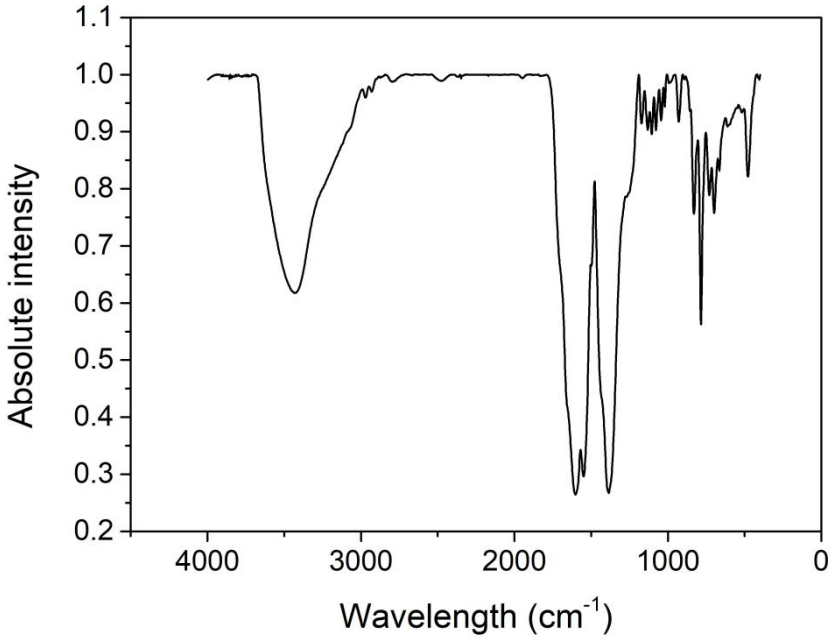

Figure S1. IR spectra of as-synthesized NUC-7.

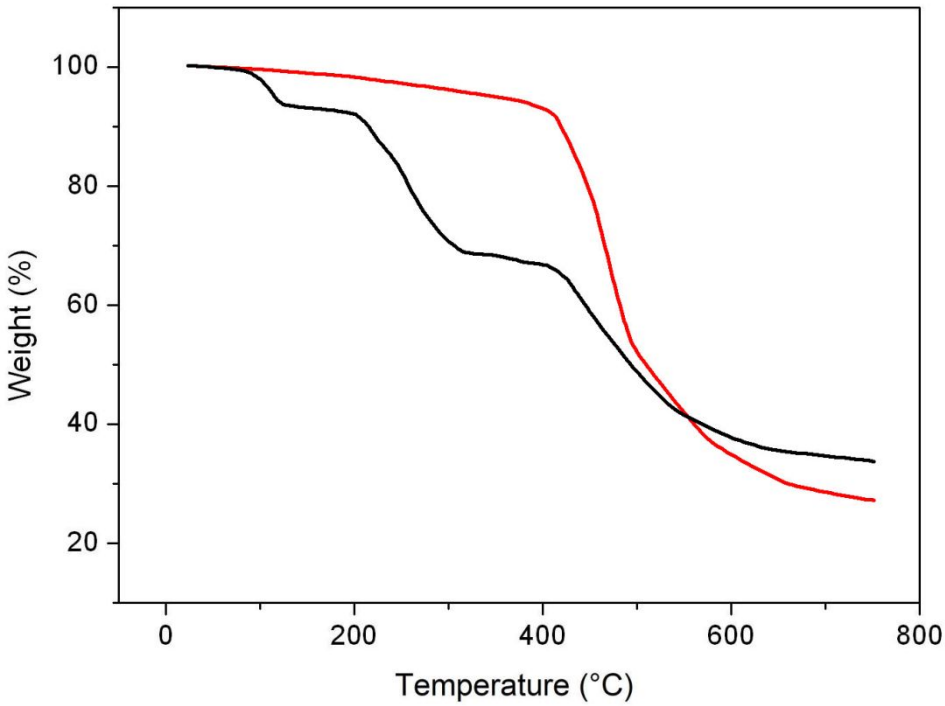

Figure S2. The TGA curves of as-synthesized (black) and activated (red) sample of NUC-7.

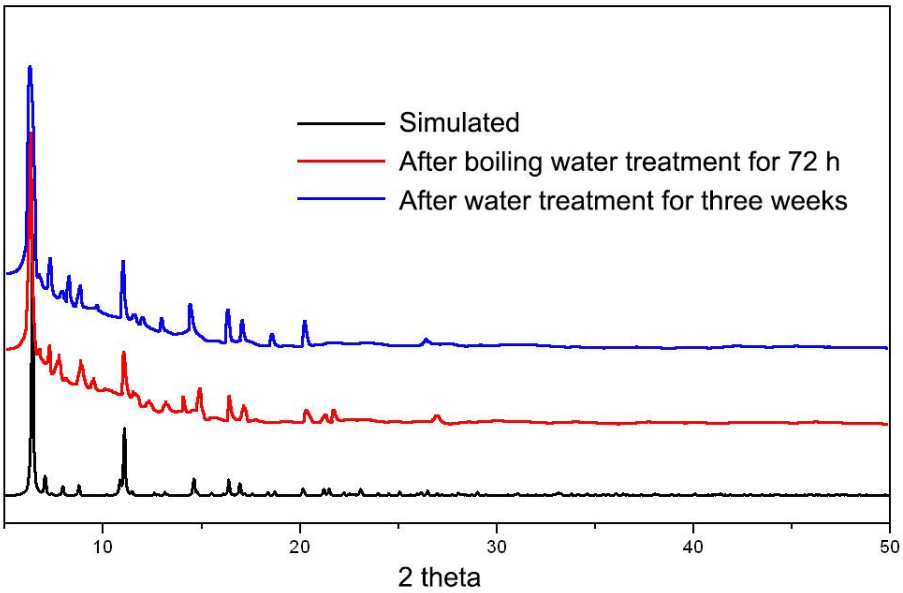

Figure S3. PXRD patterns of NUC-7 after water treatment.

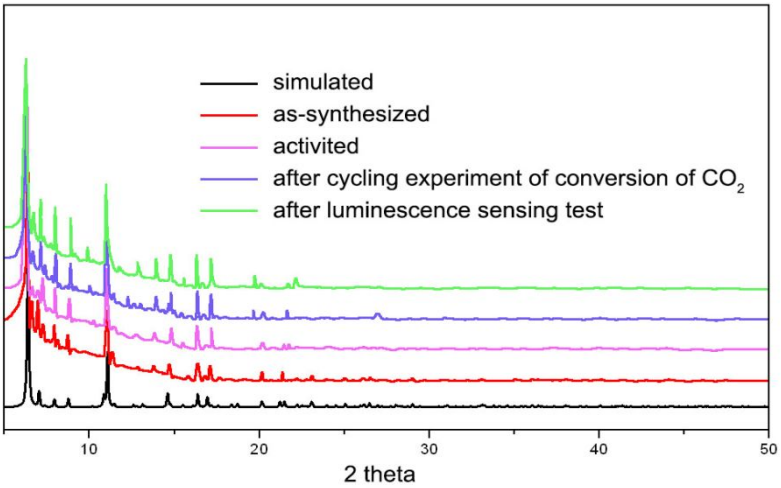

Figure S4. PXRD patterns of NUC-7

Gas adsorption

The Q_{st} value is a parameter that describes the average enthalpy of adsorption for an adsorbing gas molecule at a specific surface coverage and is usually evaluated using two or more adsorption isotherms collected at similar temperatures. The zero-coverage isosteric heat of adsorption is evaluated by first fitting the temperature-dependent isotherm data to a virial-type expression, which can be written as:

$$\ln P = \ln N + \frac{1}{T}\sum_{i=0}^{m} a_i N^i + \sum_{i=0}^{n} b_i N^i$$

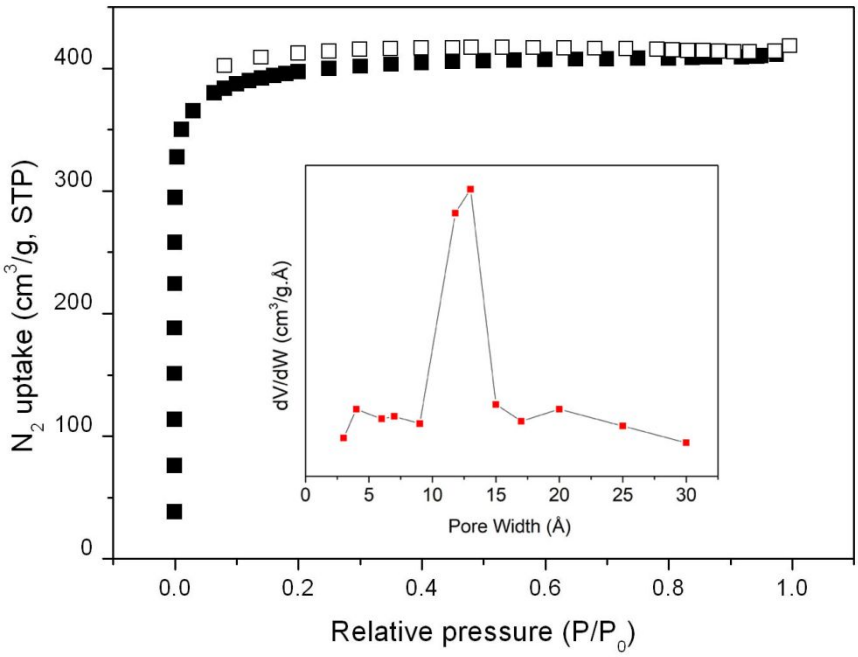

Figure S5. N_2 adsorption/desorption isotherms of NUC-7 at 77 K (Insert: the pore size distribution)

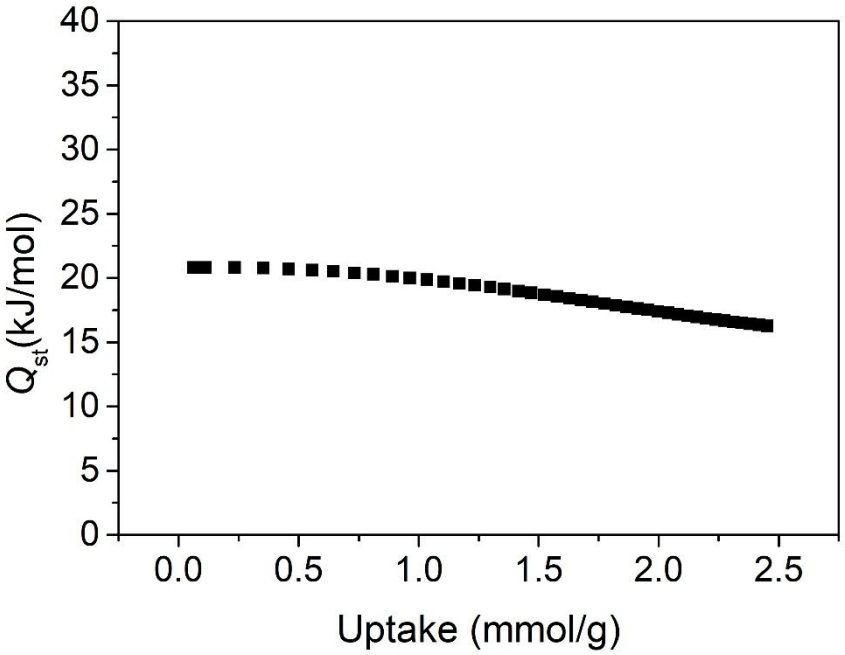

Figure S6. The adsorption heats of NUC-7 for CO_2.

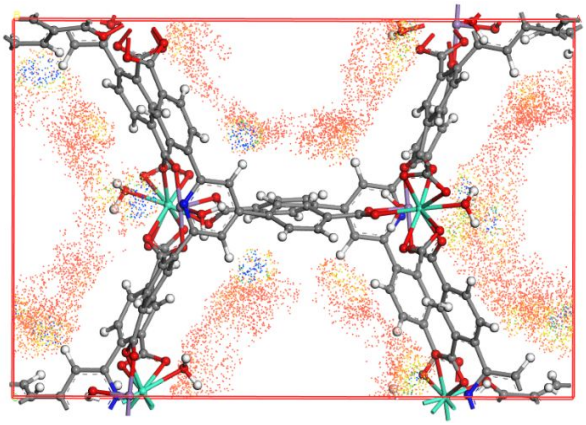

Figure S7. The simulated density distribution of CO_2 in NUC-7 at 298 K and 100 kPa. Where, red=O, blue=N, purple=Zn, green=Tb, while=H, grey=C, the 'color dots' denoted the size of density distribution.

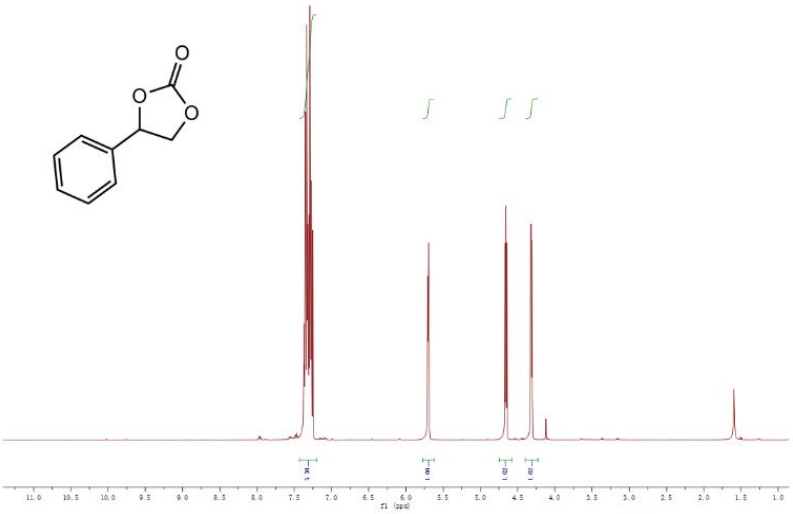

Figure S8. The ^{1}H NMR spectrum of 4-phenyl-1,3-dioxolan-2-one (Table 1).

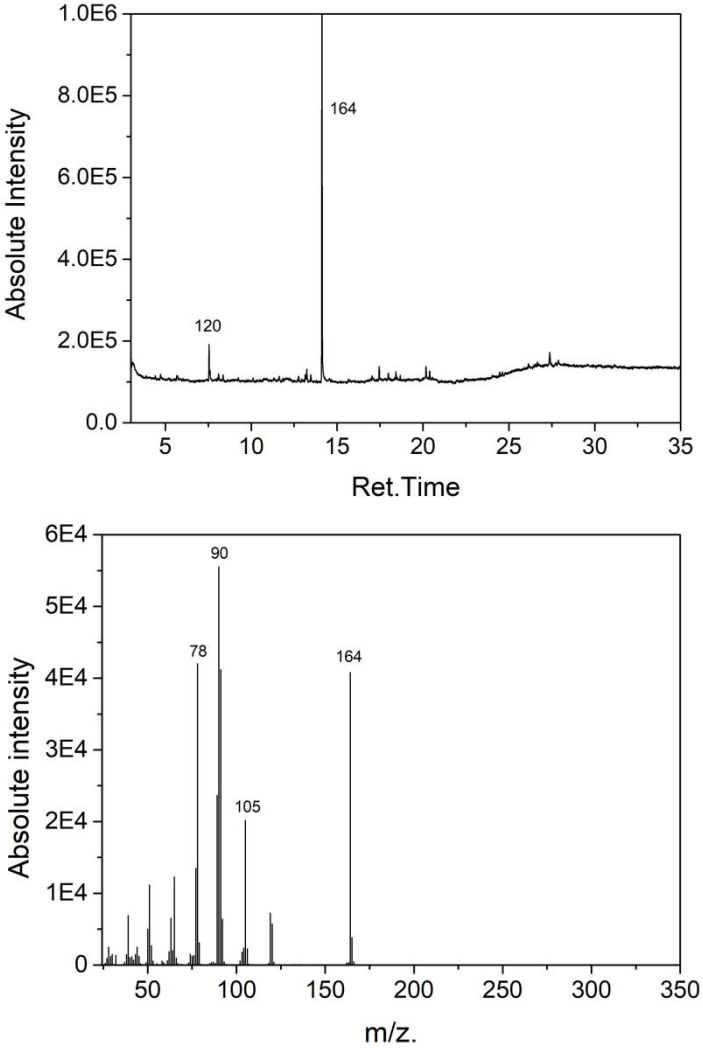

Figure S9. The GC-MS of 4-phenyl-1,3-dioxolan-2-one (entry 6, Table 1).

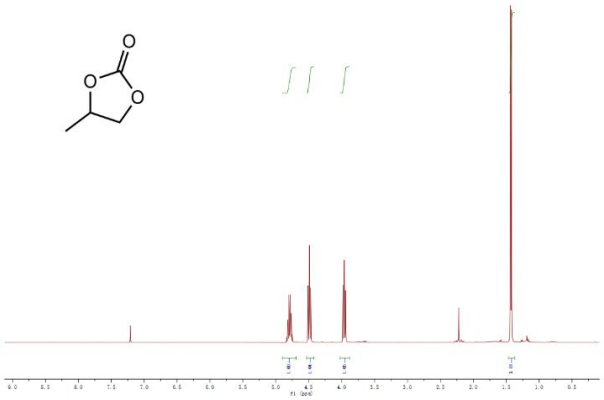

Figure S10. The ^{1}H NMR spectrum of 4-Methyl-1,3-dioxolan-2-one (Table 2, entry 1).

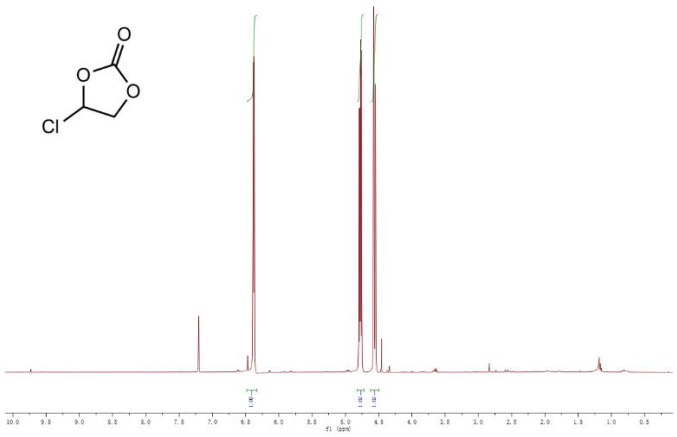

Figure S11. The ^{1}H NMR spectrum of 4-chloro-1,3-dioxolan-2-one (Table 2, entry 2).

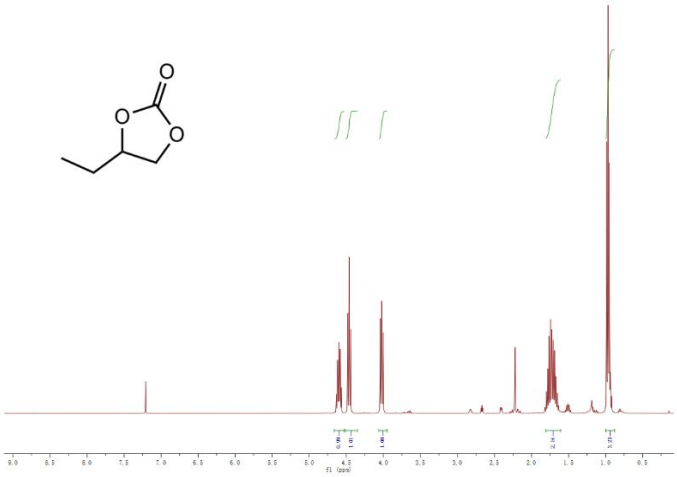

Figure S12. The ^{1}H NMR spectrum of4-ethyl-1,3-dioxolan-2-one(Table 2, entry 3).

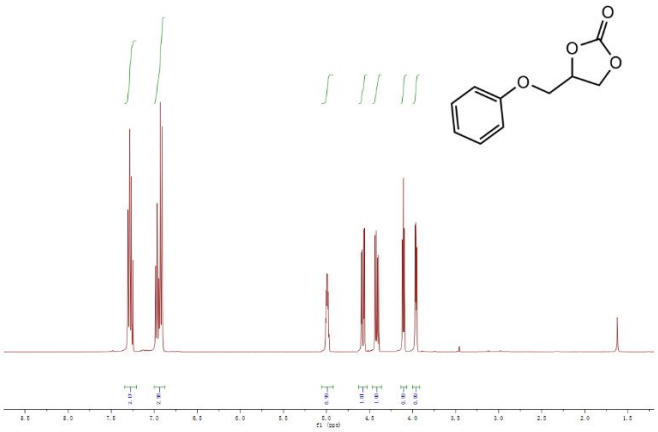

Figure S13. The ^{1}H NMR spectrum of 4-(Phenoxymethyl)-1,3-dioxolan-2-one (Table 2, entry 5).

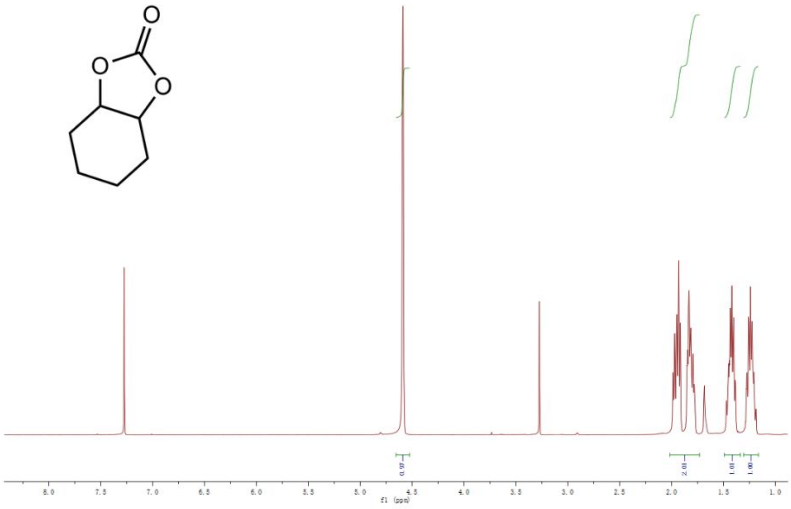

Figure S14. The ^{1}H NMR spectrum of hexahydrobenzo[d][1,3]dioxol-2-one(Table 2, entry 6).

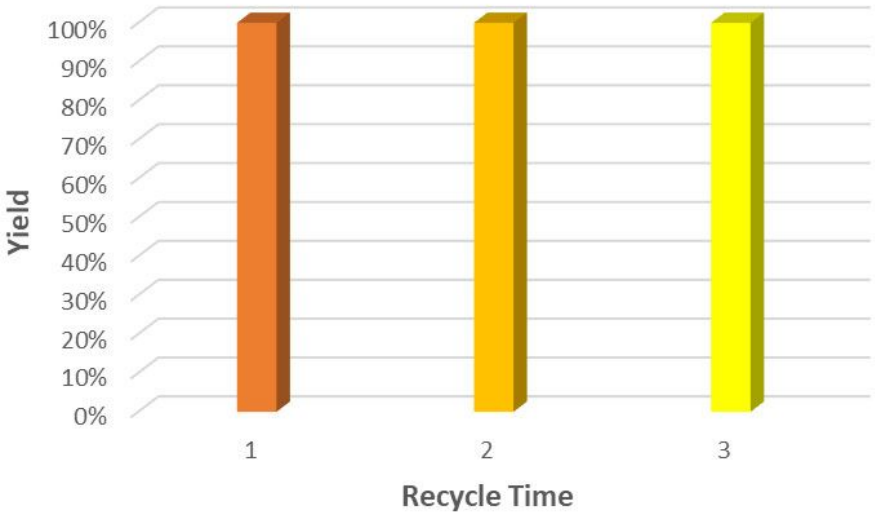

Figure S15. The reusability of NUC-7 at different catalytic cycles

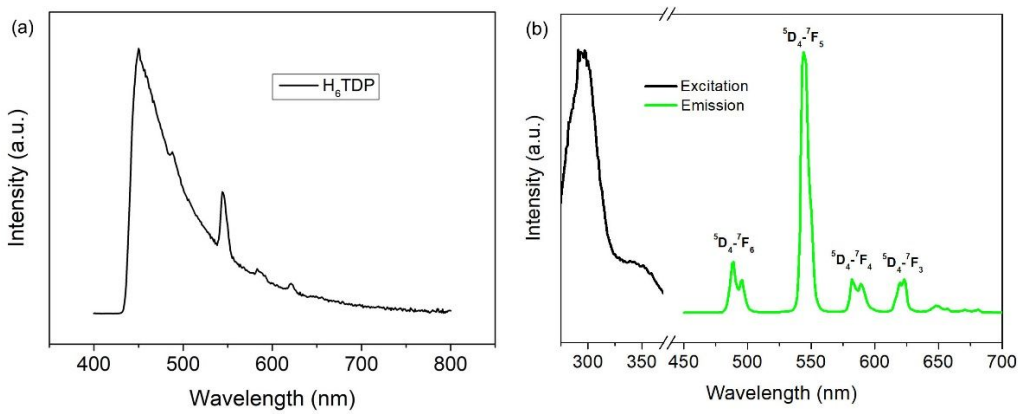

Figure S16. Luminescence spectra of free H_6TDP ligand (a) and NUC-7 (b).

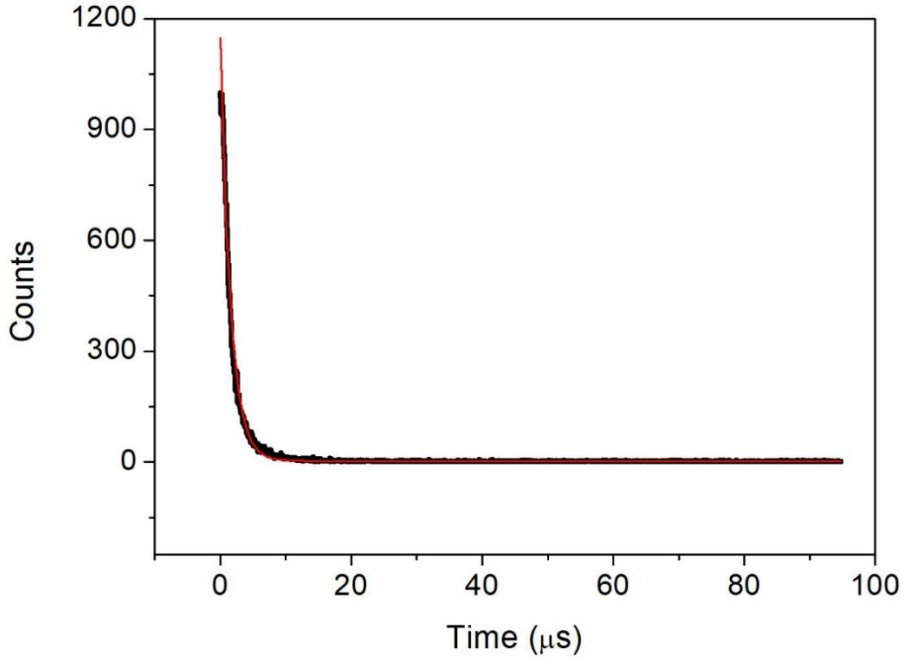

Figure S17. Luminescence decay curve of NUC-7.

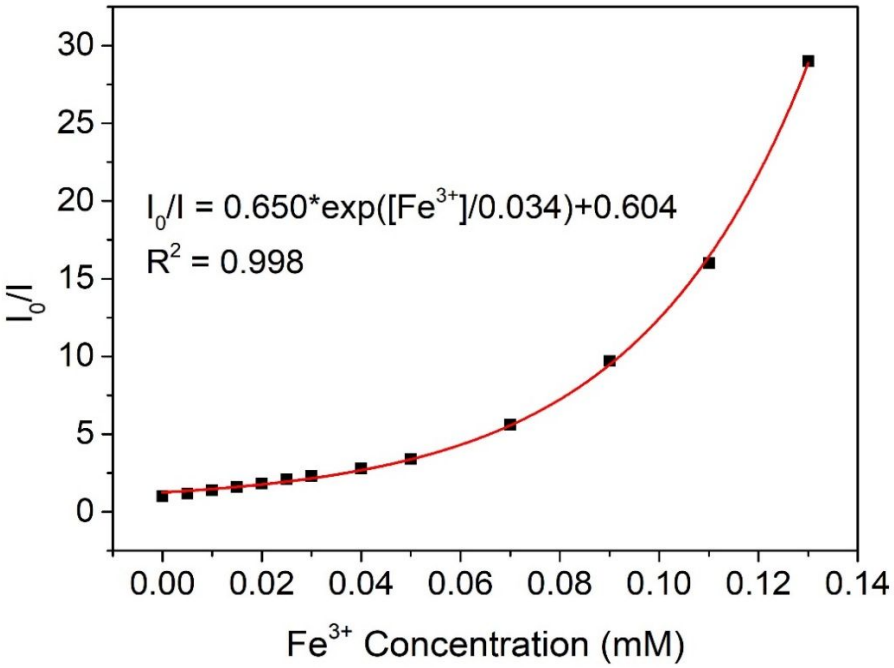

Figure S18. Luminescence intensity ratio *vs* the concentration of Fe^{3+} plot

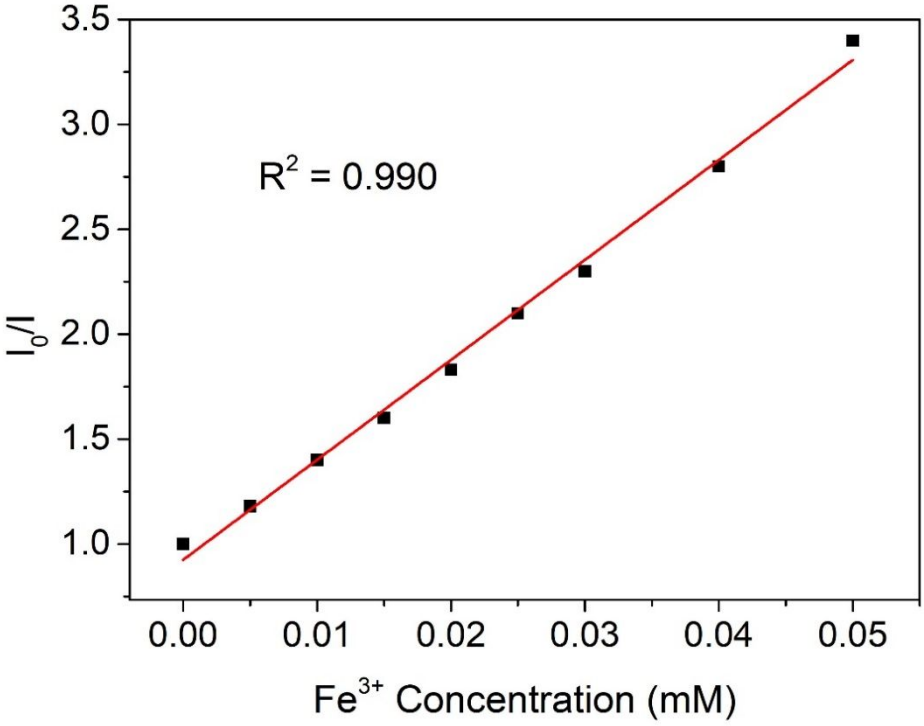

Figure S19. The luminescence intensity ratio of NUC-7 versus Fe^{3+} concentration in the range of 0 − 0.5 mM

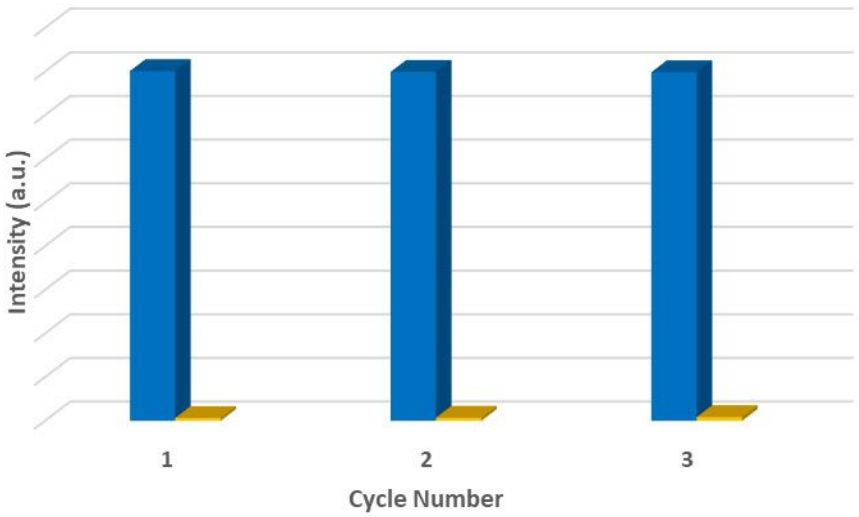

Figure S20. Luminescence quenching efficiency of NUC-7 toward Fe^{3+} after three cycles.

References

S1. Guo, X. Y.; Zhou, Z.; Chen, C.; Bai, J. F.; He, C.; Duan, C. Y. New rht-Type Metal−Organic Frameworks Decorated with Acylamide Groups for Efficient Carbon Dioxide Capture and Chemical Fixation from Raw Power Plant Flue Gas. *ACS Appl. Mater. Interfaces* **2016**, *8*, 31746−31756.

S2. Gupta, V.; Mandal, S. K. A Microporous Metal−Organic Framework Catalyst for Solvent-free Strecker Reaction and CO_2 Fixation at Ambient Conditions. https://dx.doi.org/10.1021/acs.inorgchem.9b03051.

S3. Xue, Y. S.; Cheng, W. W.; Luo, X. M.; Cao, J. P.; Xu, Y. Multifunctional Polymolybdate-Based Metal−Organic Framework as an Efficient Catalyst for the CO_2 Cycloaddition and as the Anode of a Lithium-Ion Battery. *Inorg. Chem*. **2019**, *58*, 13058−13065.

S4. Liu, J.; Hang, M.; Wu, D.; Jin, J.; Cheng, J. G.; Yang, G. P.; Wang, Y. Y. Fine-Tuning the Porosities of the Entangled Isostructural Zn(II)-Based Metal−Organic Frameworks with Active Sites by Introducing Different N-Auxiliary Ligands: Selective Gas Sorption and Efficient CO_2 Conversion. *Inorg. Chem*. **2020**, 59, 2450−2457.

S5. Babu, R.; Roshan, R.; Kathalikkattil, A. C.; Kim, D. W.; Park, D. W.; Rapid, Microwave-Assisted Synthesis of Cubic, Three-Dimensional, Highly Porous MOF-205 for Room Temperature CO_2 Fixation via Cyclic Carbonate Synthesis. *ACS Appl. Mater. Interfaces* **2016**, *8*, 33723−33731.

S6. Yao, C. Zhou, S. L.; Kang, X. j.; Zhao, Y.; Yan, R.; Zhang, Y.; Wen, L. L.; Cationic Zinc−Organic Framework with Lewis Acidic and Basic Bifunctional Sites as an Efficient Solvent-Free Catalyst: CO_2 Fixation and Knoevenagel Condensation Reaction. *Inorg. Chem*. **2018**, *57*, 11157−11164.

S7. Li, Y. X.; Zhang, X.; Lan, J. W.; Xu, P.; Sun, J. M. Porous Zn(Bmic)(AT) MOF with Abundant Amino Groups and Open Metal Sites for Efficient Capture and Transformation of CO_2, *Inorg. Chem*. **2019**, *58*, 13917−13926.

S8. Wang, J.; Jiang, M.; Yan, L.; Peng, R, Huang, F.; Guo, X.; Li, Y.; Wu, P. Multifunctional Luminescent Eu(III)-Based Metal−Organic Framework for Sensing Methanol and Detection and Adsorption of Fe(III) Ions in Aqueous Solution. *Inorg. Chem*. **2016**, *55*, 12660−12668.

S9. Yan, W.; Zhang, C.; Chen, S.; Han, L.; Zheng, H. Two Lanthanide Metal−Organic Frameworks as Remarkably Selective and Sensitive Bifunctional Luminescence Sensor for Metal Ions and Small Organic Molecules. *ACS Appl. Mater. Interfaces* **2017**, *9*, 1629−1634.

S10. Zhang, Q.; Wang, J.; Kirillov, A. M.; Dou, W.; Xu, C.; Xu, C.; Yang, L.; Fang, R.; Liu, W. Multifunctional Ln−MOF Luminescent Probe for Efficient Sensing of Fe^{3+}, Ce^{3+}, and Acetone. *ACS Appl. Mater. Interfaces* **2018**, *10*, 23976−23986.

S11. Mi, X.; Sheng, D.; Yu, Y.; Wang, Y.; Zhao, L.; Lu, J.; Li, Y.; Li, D.; Dou, J.; Duan, J.; Wang S. Tunable Light Emission and Multiresponsive Luminescent Sensitivities in Aqueous Solutions of Two Series of Lanthanide Metal−Organic Frameworks Based on Structurally Related Ligands. *ACS Appl. Mater. Interfaces* **2019**, *11*, 7914−7926.

S12. Zhang, H.; Fan, R.; Chen, W.; Fan, J.; Dong, Y.; Song, Y.; Du, X.; Wang, P.; Yang, Y. 3D Lanthanide Metal−Organic Frameworks Based on Mono - , Tri - ,and Heterometallic Tetranuclear Clusters as Highly Selective and Sensitive Luminescent Sensor for Fe^{3+} and Cu^{2+} Ions. *Cryst. Growth Des*. **2016**, *16*, 5429−5440.